Hindawi
Advances in Civil Engineering
Volume 2022, Article ID 5496999, 13 pages
https://doi.org/10.1155/2022/5496999

Research Article

Study on Deformation Characteristics of Extended Highway in Operation Period

Pengfei Zhou,[1] **Lizhuang Cui**,[2] **Xuesen Zhang**,[2] **Chuanyi Ma**,[1] **Jian Liu**,[2] **Yanni Shao**,[3] **Gaohang Lv**,[3] **and Quanyi Xie**[2]

[1]*Shandong Express Group Co., Ltd., Jinan 250061, China*
[2]*School of Qilu Transportation, Shandong University, Jinan 250002, China*
[3]*School of Civil Engineering, Shandong University, Jinan 250061, China*

Correspondence should be addressed to Quanyi Xie; quanyixiesdu@163.com

Received 19 February 2022; Revised 23 June 2022; Accepted 20 July 2022; Published 21 August 2022

Academic Editor: Giulio Dondi

Highway widening has become an effective way to improve the carrying capacity of existing expressways. However, assume that the differential settlement between the new and the old subgrades is not controlled. In that case, it will lead to longitudinal cracks on the pavement, which will seriously affect the safety of vehicles. In this study, the variations of elastic modulus and dynamic elastic modulus of new and old subgrades under traffic load were studied by tests. A hyperbolic model of dynamic elastic modulus increasing with strain is proposed. The numerical calculation model of new and old subgrades under traffic load is established. The deformation characteristics of new and old subgrades without treatment measures and setting up geogrid and geocell are studied. The main conclusions are as follows: (1) with the increase of traffic load and subgrade depth, the elastic modulus changes significantly in the early stage and small in the later stage. (2) Under the condition of no treatment measures, the vertical and horizontal deformation of the subgrade surface show a trend of increasing and then decreasing with the distance from the center line of the subgrade. (3) Setting geogrid and geocell can effectively reduce the differential settlement of the old and new subgrades. (4) The effect of setting geogrid to reduce the differential settlement of old and new subgrades is better than that of setting geogrid.

1. Introduction

Expressways have become the main infrastructure for inter-regional transportation due to their advantages, such as fast speed, high efficiency, and large carrying capacity. With economic development and increasing traffic volume, the number of lanes on some expressways can no longer meet the demand for transportation [1–7]. Highway widening has become one of the effective solutions. The old expressway subgrade has undergone long-term traffic operation, and the compression deformation has been stable [8]. The new subgrade will still undergo large compression deformation under the action of traffic load [9–11]. If the differential settlement between the new and old subgrades is not controlled, it will cause longitudinal cracks on the road surface, affecting vehicles' safety seriously [12].

The dynamic triaxial test has become one of the main methods to research the dynamic deformation characteristics of the soil [13–15]. The dynamic characteristics of subgrade soil structure have been studied in order to meet the design requirements of complex practical engineering [16–18]. In the early stage, the experimental study of dynamic characteristics was mainly based on seismic load, characterized by high confining pressure, significant strain, and few cycles [19, 20]. Experimental research has been carried out on the deformation characteristics under the traffic load by using dynamic triaxial tests and resonance column tests [21–24]. However, the existing research still has some shortcomings in restoring the operation state of the old and new subgrades, and the performance comparison of the two subgrades has not been achieved. Numerical calculation has been carried out to research the dynamic response characteristics of subgrade under the traffic load by relying

on actual engineering [25–27]. Moreover, under traffic load, the differential deformation rule of the new and old subgrades of the Yellow River flooding area has not been systematically revealed, which seriously hinders the progress of the Yellow River extension expressway reconstruction project.

Therefore, the mechanical properties of subgrade filling soil in the Yellow River extension are studied in this study based on the Bin-Lai Expressway expansion project in the Yellow River extension. The traffic load action in the Yellow River extension is quantified. The dynamic triaxial test is carried out to study the dynamic characteristics of new and old subgrades soil in the Yellow River extension. The numerical calculation model of dynamic settlement of new and old subgrades under traffic load is established. The differential deformation rule of new and old subgrades is studied, providing theoretical and data support for highway extension design in the Yellow River extension.

2. Laboratory Experiment

2.1. Testing Device. The Eldyn dynamic triaxial apparatus is used as the test device, as shown in Figure 1. The equipment can provide the cyclic loading mode of force control or displacement control. The maximum axial force is 5 kN, the maximum loading frequency is 5 Hz, and the maximum confining pressure is 1 MPa. The data acquisition system of the equipment can collect pore water pressure, strain, axial force, back pressure, and back pressure volume. The accuracy of pore water pressure and back pressure sensor is 1 kPa, the accuracy of back pressure volume is 1 mm^3, and the accuracy of axial force is 1 N.

2.2. Test Materials. In this test, a representative dynamic triaxial test of subgrade soil samples was selected. The soil used in the test was taken from the extension project from Zibo West to the Laiwu section of the Bin-Lai Expressway. The optimum water content was obtained by the Proctor compaction. The liquid plastic limit was determined by the liquid plastic limit tester. Soil samples' cohesion and internal friction angle were measured by the triaxial compression test. The soil properties of the testing samples are listed in Table 1.

2.3. Experimental Conditions. The test conditions set for this test is listed in Table 2. First, the dynamic characteristics of subgrade soil at different depths and vehicles were obtained by dynamic loading tests under conditions I, II, and III. After completing the dynamic loading test, the sample was used as the old subgrades for subsequent mechanical characteristics research. Then, the elastic modulus, shear modulus, internal friction angle, and cohesion were tested for conditions I, II, III, and IV. Among them, the samples with stable deformation after the dynamic loading test are regarded as old subgrade, the nine samples in test conditions I, II, and III. The newly prepared samples without dynamic cycle were considered the new subgrade soil, namely, the three samples in test condition IV.

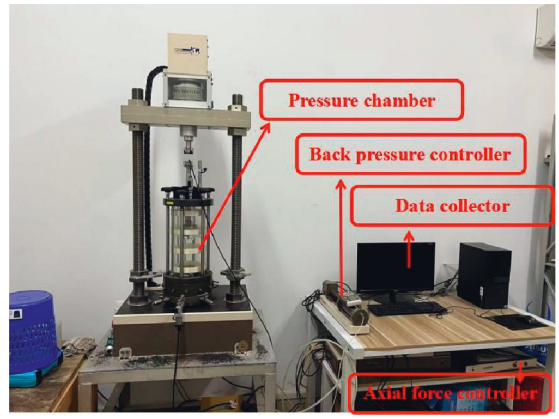

Figure 1: Eldyn dynamic triaxial apparatus.

2.4. Experiment Procedure

(1) *Pretreatment of Soil Samples.* The soil samples were dried, crushed, and passed through a 2 mm screen. After screening, add water to the soil sample to the optimal moisture content and seal it in a plastic bag for 24 hours.

(2) *Triaxial Sample Making.* Coat a vaseline layer evenly on the inner wall of sample cylinder (50 mm × 100 mm). Then, the prepared soil sample is smashed into the compacting instrument in five layers, and vacuum saturation is conducted on the prepared triaxial sample.

(3) *Saturation Test of a Triaxial Sample.* Install the sample on the base of the triaxial test instrument. The ratio of pore pressure increment to confining pressure increment after applying confining pressure is taken as the evaluation index of saturation. If the saturation reaches more than 0.95, the triaxial test is directly started; if the saturation is less than 0.95, the backpressure is applied on the top of the sample until the saturation reaches 0.95.

(4) *Sample Consolidation.* Isobaric consolidation is adopted in this test, and isobaric lateral and axial pressures are applied to the samples. The standard for completion of the consolidation stage is that the change of consolidation displacement does not exceed 0.1 cm^3 within 1 h.

(5) *Application of Dynamic Load to the Sample.* The dynamic load is applied to the sample according to the test design condition, and the variations of soil deformation, pore pressure, and other parameters are monitored.

(6) After the sample's axial strain and pore pressure remain stable under dynamic load, the sample's shear and elastic modulus are tested under the corresponding state.

2.5. Dynamic Modulus Attenuation Rule. The dynamic stress-dynamic strain curve of the soil can be fitted to a hyperbolic type, which can be expressed by the following equation:

Table 1: Basic material parameters of subgrade soil.

Maximum dry density (g/cm^3)	Liquid limit (%)	Plastic limit (%)	Plasticity index	Optimum water content (%)	Cohesion (kPa)	Internal friction angle (°)
1.76	36.96	18.20	8.7	17.03	4.59	31

Table 2: Test conditions.

Working condition	Borrow depth (m)	Confining pressure (kPa)	Wheel axle weight (kN)	Dynamic stress (kPa)	Frequency (Hz)
I-1	—	—	50	4.2	—
I-2	0.5	14	130	11.0	—
I-3	—	—	240	20.2	—
II-1	—	—	50	1.2	—
II-2	1.5	24	130	3.2	1
II-3	—	—	240	6.0	—
III-1	—	—	50	0.6	—
III-2	2.5	34	130	1.5	—
III-3	—	—	250	3.0	—

$$\sigma_d = \frac{\varepsilon_d}{b + a\varepsilon_d}, \tag{1}$$

where σ_d is dynamic stress and ε_d is dynamic strain.

According to equation (1), dynamic elastic modulus can also be expressed as follows:

$$E_d = \frac{1}{b + a\varepsilon_d}. \tag{2}$$

It can be seen from equation (2) that the change curve of $1/E_d - \varepsilon_d$ can be fitted to a linear. In order to facilitate data sorting and analysis, the maximum dynamic modulus $E_{d\max}$ is introduced here to normalize the dynamic modulus E_d, which is as follows:

$$\frac{E_{d\max}}{E_d} = 1 + \frac{a}{b}\varepsilon_d. \tag{3}$$

During the test process, under the action of dynamic loads at each depth, three samples were prepared for each working condition, and the same test conditions (the same confining pressure and dynamic stress) were applied. The scatter plots of three samples' test results were reflected in the coordinate system. The relationship between $E_{d\max}/E_d$ and ε_d is obtained by linear fitting equation (equation (3)). Furthermore, the dynamic modulus-dynamic strain fitting curve drawn is shown in Figure 2.

It can be seen from the figure that the relationship between $E_{d\max}/E_d$ and ε_d is roughly in line with the linear fitting relationship, and the fitting variance is around 0.95, indicating that the fitting relationship is reliable. The test results are subject to human interference factors, such as soil water addition, sample compaction, vacuum saturation, and some discrete data generated by individual working conditions. Still, they do not affect the overall trend of change. Strictly speaking, the intercept should be 1. However, $E_{d\max}$ is obtained by the mathematical limit idea and is not an accurate value, so the straight line is intercepted on the vertical axis. The distance floats around the value 1, with a slight deviation; the slope of the straight line expressed as a/b is $E_{d\max}/\sigma_{d\max}$, and the change of the slope is affected by the magnitude of the dynamic load, as listed in Table 3. The axle load increased from 50 kN to 240 kN, the slope at a depth of 0.5 m was reduced from 31.9 to 20.1, and the slope at a 2.5 m depth decreased from 41.3 to 37.1. The larger the dynamic load of subgrade soil is, the smaller the slope of the fitting straight line is. The load affects the subgrade surface with a depth of less than 0.5 m. With the increase of depth, the slope of the straight line is less affected by the dynamic load.

2.6. Result Analysis of Mechanical Characteristics of New and Old Subgrades. In this study, samples with stable deformation under dynamic load were used as old subgrade to test elastic modulus and shear modulus. It can be seen from Figures 3 and 4 that the distribution rule of elastic modulus and shear modulus of new and old highway subgrades is the same. At each depth, the modulus of the old subgrade after experiencing the different traffic cycle loads increases to different degrees compared with that of the new subgrade. The largest is the elastic and shear modulus of the old subgrade subjected to load $P_n = 50$ kN. As the traffic load increases, the modulus of the old subgrade decreases. Under the same traffic load, the elastic modulus and shear modulus of the new and old subgrades both increase in varying degrees with increasing depth. It can be seen that whether it is with the increase of the traffic load or the increase of the depth, the modulus changes show a trend of significant changes in the early period and small changes in the later period.

3. Numerical Calculation Analysis

3.1. Numerical Calculation Model. Bin-Lai Expressway in Shandong province was used as the numerical simulation object in this study. Bin-Lai Expressway is the first north-south expressway in Shandong that runs through mountainous areas. With the rapid development of society, there are more and more traffic volume and full load transportation phenomena on expressways. The number

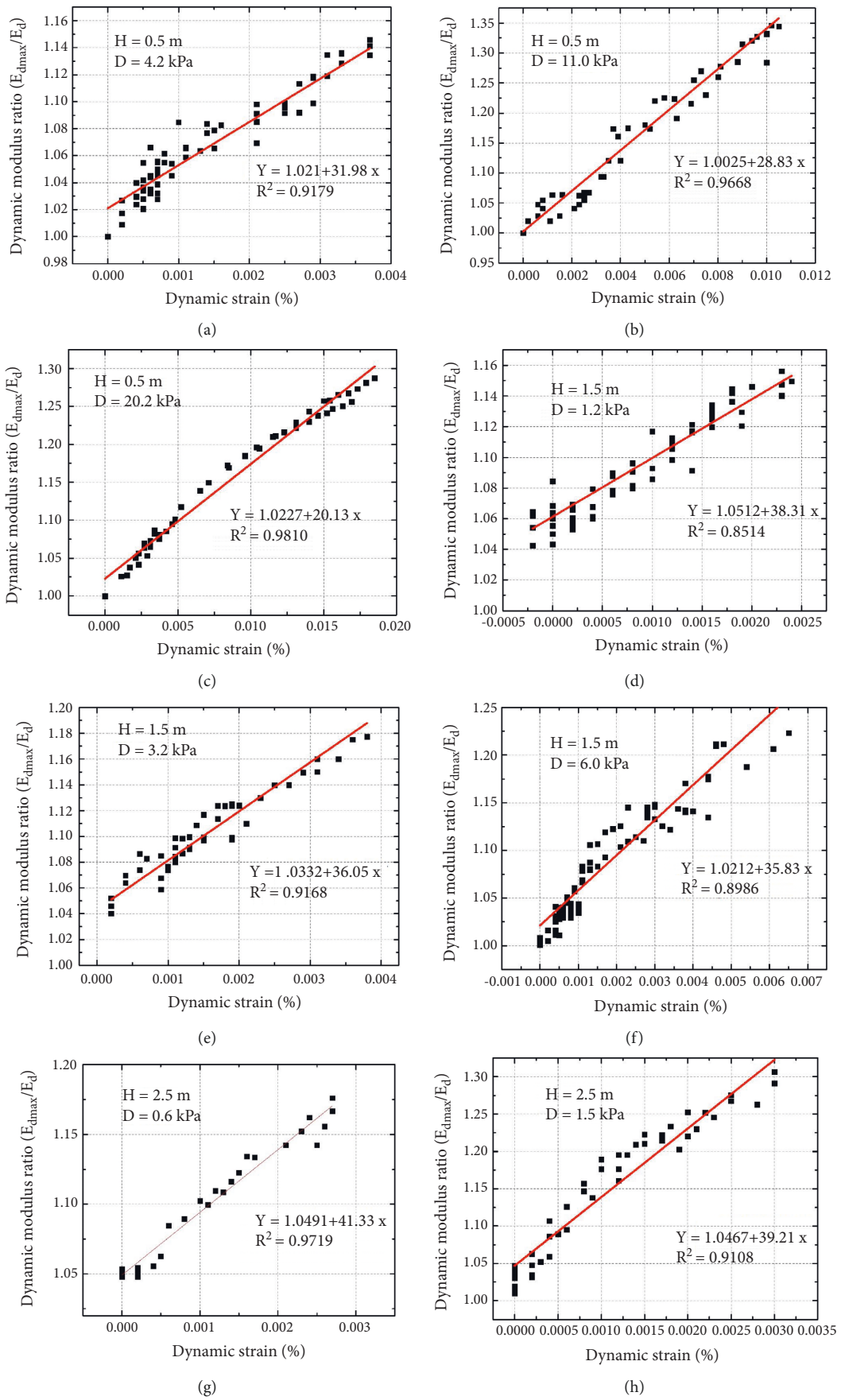

Figure 2: Continued.

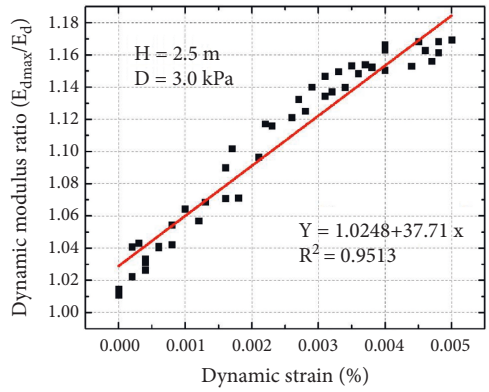

(i)

Figure 2: Dynamic modulus ratio-dynamic strain fitting curve. (a) $H = 0.5$ m, $D = 4.2$ kPa. (b) $H = 0.5$ m, $D = 11.0$ kPa. (c) $H = 0.5$ m, $D = 20.2$ kPa. (d) $H = 1.5$ m, $D = 1.2$ kPa. (e) $H = 1.5$ m, $D = 3.2$ kPa. (f) $H = 1.5$ m, $D = 6.0$ kPa. (g) $H = 2.5$ m, $D = 0.6$ kPa. (h) $H = 2.5$ m, $D = 1.5$ kPa. (i) $H = 2.5$ m, $D = 3.0$ kPa.

Table 3: Slope (a/b).

Depth (m)	Axle load 50 kN	Axle load 130 kN	Axle load 240 kN
0.5	31.9	28.8	20.1
1.5	38.3	36.0	35.8
2.5	41.3	39.2	37.1

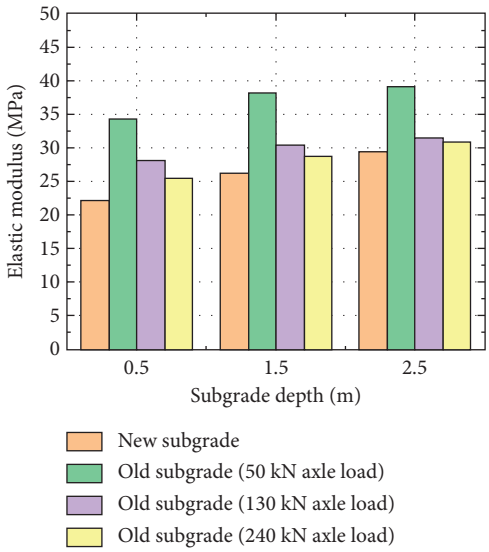

Figure 3: Elastic modulus comparison.

of highway lanes can no longer meet the demand for transportation, and the original roads must be widened. Bin-Lai Expressway plans to expand the original two-way four-lane road from Zibo West to Laiwu section of the Bin-Lai Expressway into a two-way eight-lane road by widening and building on both sides. After the section is widened, the entire width of the road is set to 42 m, and the driving speed is 120 km/h. The standard cross-section of integrated subgrade widened on both sides is shown in Figure 4.

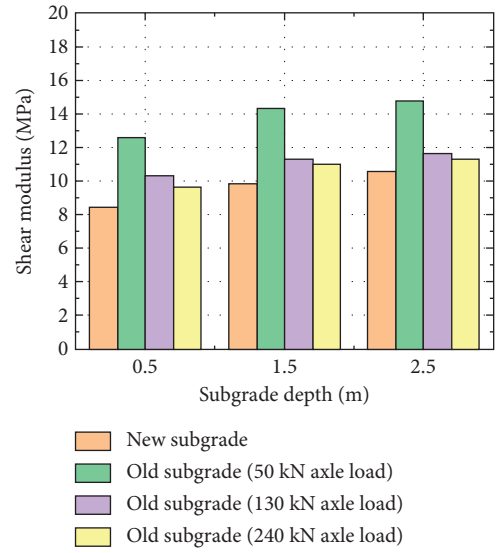

Figure 4: Shear modulus comparison.

This model takes advantage of the symmetry of the widened subgrade on both sides, taking the center of the old subgrade as the axis of symmetry to take half of the subgrade for simulation analysis. The calculated size of the subgrade is as follows: width × depth: 21 m × 3 m, of which the size of the old subgrade is 9.75 m × 3 m, the size of the new subgrade is 11.75 m × 3 m, the old and new subgrades are equally filled in three layers, and the subgrade slope ratio is 1 : 1.5; the calculated foundation size is as follows: width × depth: 35.5 m × 14 m, and the model adopts three-dimensional elements and 30,602 nodes. The distribution of the soil layers of the new and old subgrades is shown in Figure 5.

The material parameters used in ABAQUS numerical simulation were determined by triaxial tests. The elastic modulus, Poisson's ratio, cohesion, and internal friction angle at different depths of the new and old subgrades were obtained from previous tests. The material parameters of each soil layer are listed in Table 4.

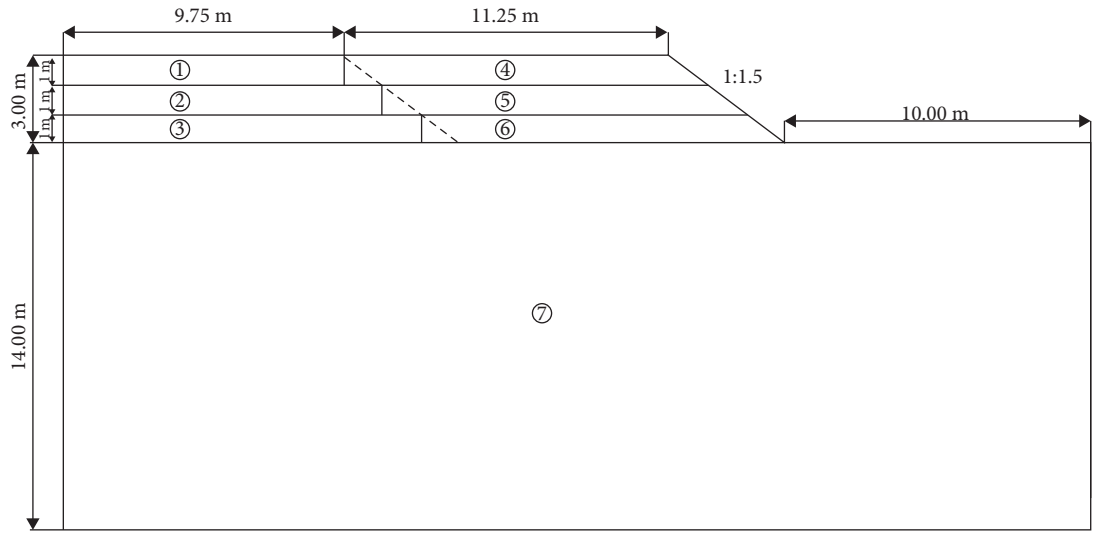

Figure 5: Schematic diagram of new and old subgrade overlapping.

Table 4: Material parameters of each soil layer.

Soil layer distribution	Traffic load (kN)	Density (kg/m^3)	Elastic modulus (MPa)	Shear modulus (MPa)	Poisson's ratio	Cohesion (kPa)	Internal friction angle (°)
Old subgrade ①	—	—	34.3	12.5	0.36	5.889	30
Old subgrade ②	—	—	38.2	14.3	0.34	5.889	30
Old subgrade ③	50	1760	39.2	14.7	0.33	5.889	30
New subgrade ④	100	—	22.5	8.4	0.33	4.585	31
New subgrade ⑤	200	—	26.1	9.7	0.34	4.585	31
New subgrade ⑥	—	—	29.3	10.6	0.36	4.585	31
Foundation ⑦	—	1840	35.0	13.5	0.30	5.0	35

3.2. Numerical Calculation Conditions. Three types of test conditions have been set in this study, as listed in Table 5. The condition without treatment measures is mainly to research the differential deformation characteristics of the new and old subgrades without any reinforcement measures. The two working conditions of geogrid and geocell mainly analyze the effect of geogrid and geocell on reducing the differential deformation of the old and new subgrades. The geogrid is used to research the deformation characteristics of the new and old subgrades when the 1st, 3rd, 5th, and 6th floors are installed, as shown in Figure 6. The geocell is used to research the deformation characteristics of new and old subgrades when the 1st, 2nd, and 3rd floors are installed, as shown in Figure 7. It is noted that the effect of geocell and geogrid on controlling the deformation of new subgrade is studied through numerical simulation, and the reinforcement method suitable for the expansion project of the low subgrade in the plain area (i.e., subgrade with height less than 3 m) is researched, which provides data support for the subgrade expansion project.

Table 5: Numerical calculation conditions.

Conditions	Treatment measures	Layer numbers
I	No treatment measures	—
II	Geogrid	1, 3, 5, 6
III	Geocell	1, 2, 3

4. Discussion of Simulation Results of No Treatment Measures

In this study, the differential settlement between the old and new subgrades has been studied for the expansion project of the low subgrade (subgrade height less than 3 m) in the Yellow River Plain. Bin-Lai Expressway in Shandong province was used as the numerical simulation object.

4.1. Vertical Displacement. As shown in Figure 8, the consolidation trend of the settlement curve increases first and then decreases. In the old and new subgrade models, the minimum and maximum vertical displacement of road surface are at the center of the old subgrade and the central pavement of the new subgrade, respectively, and the maximum settlement difference is about 0.86 cm. The model elements below the centerline of the new road foundation and the old subgrade are taken, and the variation rule of their vertical displacement is shown in Figure 9. The settlement curves of the new and old subgrades along the depth direction are approximately linear distribution, and the settlement is the largest at the surface of the subgrade. With the increase of depth, the settlement decreases gradually, and the settlement difference between the old and new subgrades decreases with the increase of depth. By observing the slope

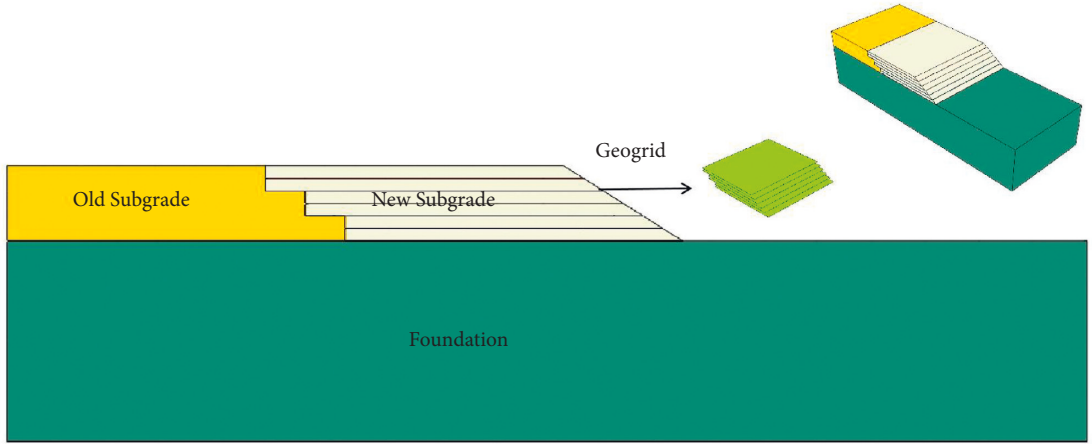

Figure 6: Geogrid.

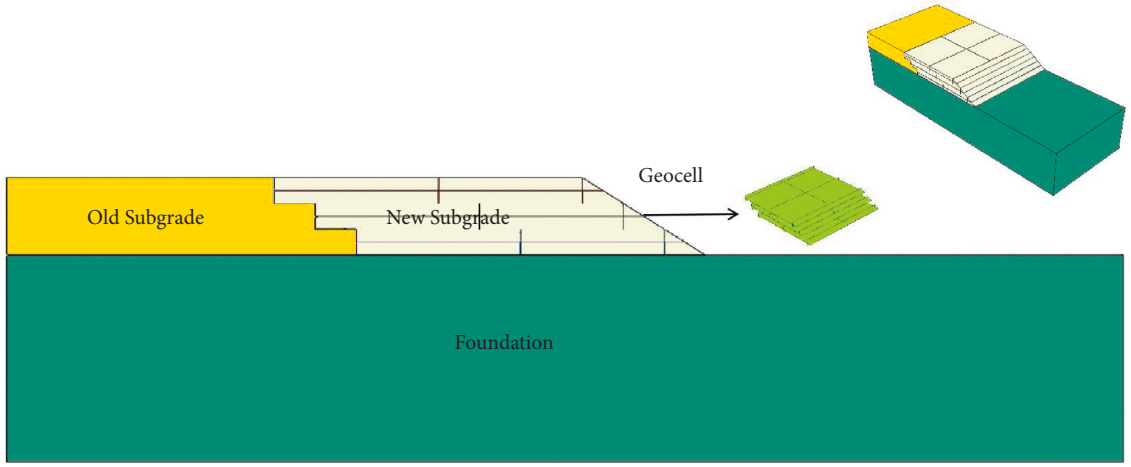

Figure 7: Geocell.

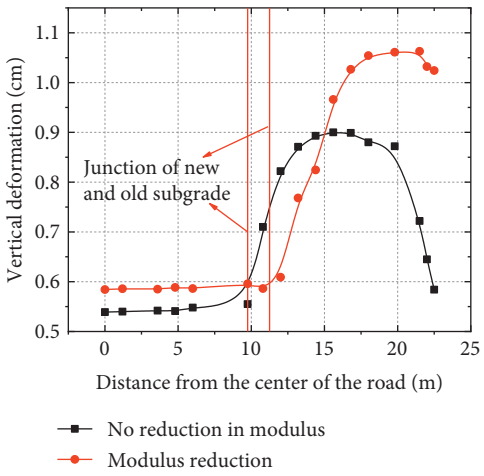

Figure 8: Subgrade surface settlement change curve.

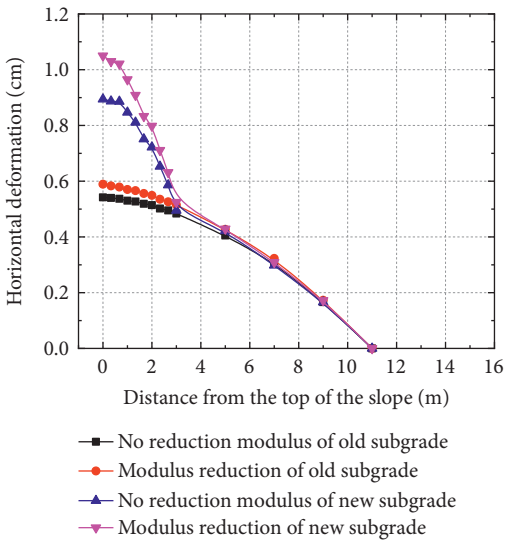

Figure 9: Settlement change curve in a depth direction of subgrade.

of the curve, it can be found that the variation range of the settlement curve of the new subgrade is more evident than that of the old subgrade. From the top of the subgrade to the depth of 3 m, the settlement of the new subgrade is reduced by 65.8% and that of the old subgrade by 51.6%. It can be seen that the deformation of the new subgrade is more affected by traffic load, and the settlement reaction is more intense at different subgrade depths.

4.2. Horizontal Displacement. It can be seen from Figure 10 that the curve changes roughly in a "reversed check" distribution. The maximum lateral deformation occurred at the joint part of the new and old subgrades, about 0.38 mm. Then, the horizontal deformation of the new subgrade decreases rapidly. It can be seen from the curve that a horizontal displacement to the right occurs from the center of the old subgrade to the direction of the new subgrade expansion. According to the symmetry of the new and old subgrades, the other side will produce horizontal displacement to the left, so it can be deduced that the center of the old subgrade will be prone to cracking due to the horizontal deformation in the opposite direction. Therefore, in the design of highway widening, reasonable width of slope and step should be selected during the excavation of the old subgrade slope to improve the shear strength at the joint and the overall stability of the subgrade and reduce the transverse deformation. The central part of the old subgrade should also be strengthened to avoid cracking after opening to traffic. The horizontal displacement curve in Figure 11 shows a trend of increasing and then decreasing, and the upper and lower deformation of the slope is roughly symmetrical. Therefore, in the new subgrade widening project, attention should be paid to the reinforcement and protection of the slope, especially in the waist of the slope, by adding geogrid, pile anchor, and other measures to reduce the deformation of the slope.

5. Discussion of Simulation Results of Geogrid

5.1. Vertical Deformation. Figure 12 shows the vertical deformation distribution law of the top surface of the subgrade along the horizontal direction. The overall vertical deformation of the old subgrade under the driving load is relatively small. From the overlapping of the old and new subgrades, the vertical deformation of the top surface of the subgrade increases first. It then decreases as the distance from the center of the subgrade increases. The peak value of the vertical deformation of the top surface of the subgrade appears at the center of the new subgrade, as shown in Figures 13 and 14. The vertical deformation of the old subgrade shows an approximately linear decrease with the increase in depth. The vertical deformation of the new subgrade shows a nonlinear decreasing trend with increasing depth. Due to the effect of the geogrid, the upper layer of the subgrade without geogrid deforms significantly, and the lower layer of the subgrade with geogrid deforms vertically. With the increase in the number of geogrids, the spatial distribution of vertical deformation shows a decreasing trend.

5.2. Horizontal Displacement. Figure 15 shows the horizontal deformation rule of the top surface of the subgrade along the horizontal direction. The horizontal deformation of the top surface of the subgrade increases first and then decreases as the distance from the center of the subgrade increases. The most significant deformation occurs in the overlap range of the old and new subgrades. With the

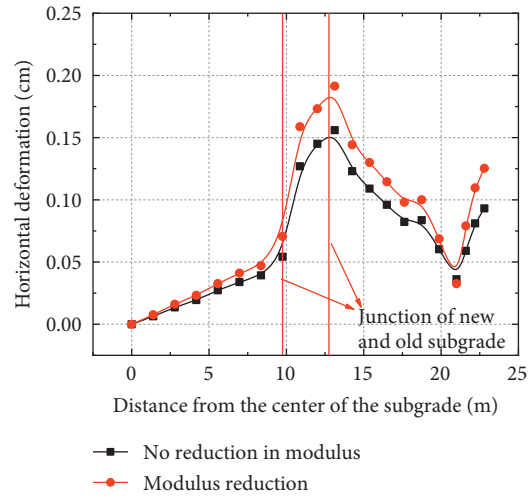

Figure 10: Horizontal displacement curve of subgrade surface.

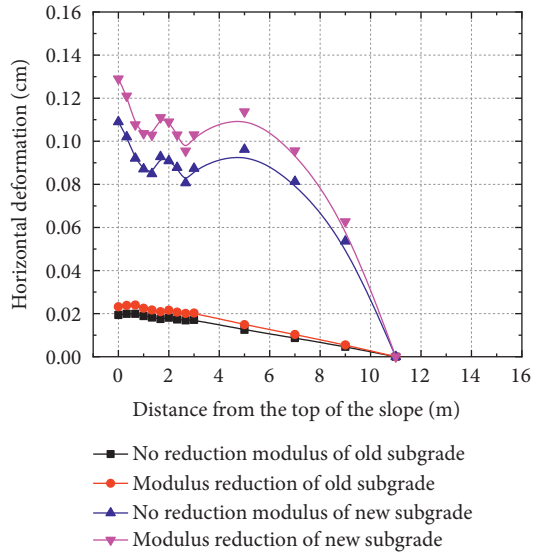

Figure 11: Horizontal displacement curve of new subgrade slope.

increase of geogrid numbers, the maximum horizontal displacement of the subgrade shows a trend of decreasing and then increasing. When the number of geogrids is increased to three layers, the geogrids are added, and the horizontal deformation of the subgrade hardly has little change.

It can be seen from Figures 16 and 17 that the deformation of the centerline of the old subgrade decreases linearly with the increase of depth. The centerline deformation of the new subgrade becomes a nonlinear decreasing trend with increasing depth. The maximum horizontal displacement on the centerline of the old subgrade is about 0.037 cm. The maximum horizontal displacement on the centerline of the new subgrade is about 0.14 cm, which is about 0.101 cm larger than the old subgrade. As the number of geogrids increases, the nonlinear trend of horizontal deformation in the vertical direction gradually becomes weaker. It shows that with the increase of geogrids, the role of subgrade resisting the traffic load is enhanced.

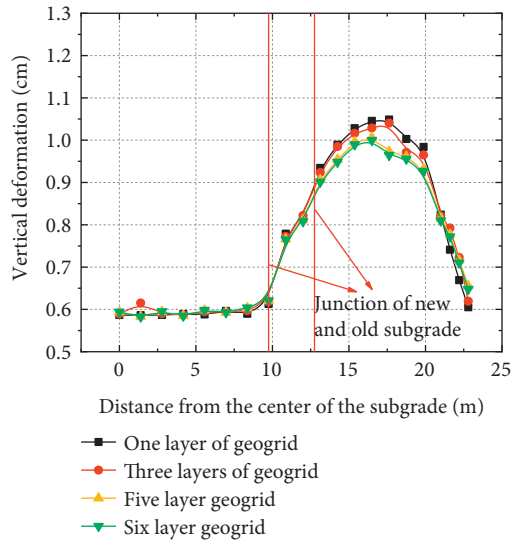

Figure 12: Vertical deformation rule of the top surface of subgrade along the horizontal.

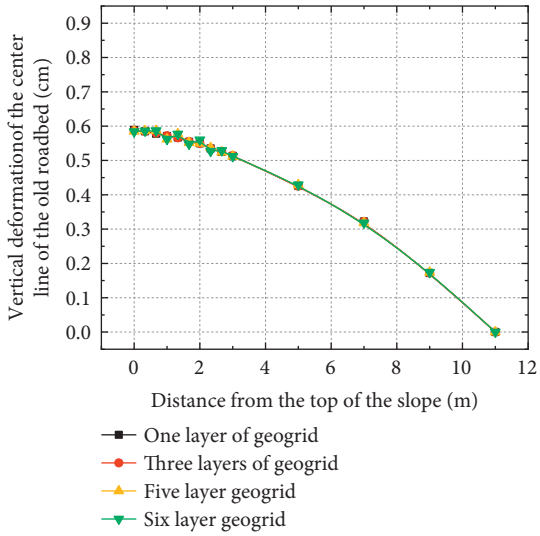

Figure 13: Vertical displacement along the depth of the center line of the old subgrade.

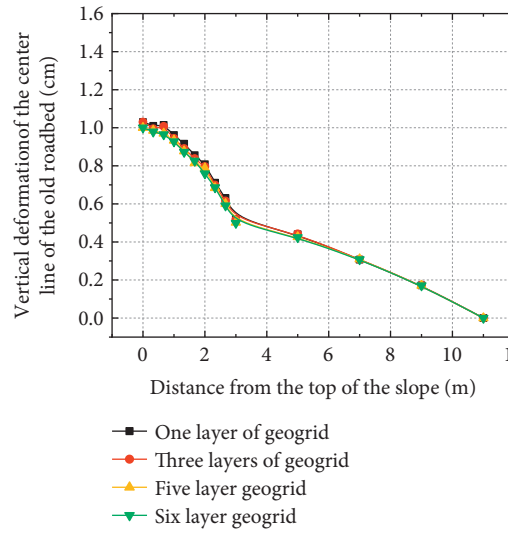

Figure 14: Vertical displacement along the depth of the center line of the new subgrade.

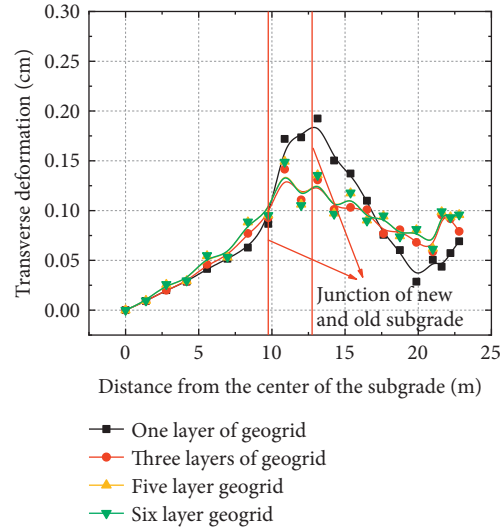

Figure 15: The rule of horizontal deformation of the top surface of subgrade along the horizontal direction.

5.3. Influence of Vehicle Number. Figures 18 and 19 show the relationship between the maximum vertical displacement and the maximum horizontal displacement of the subgrade as the number of vehicles increases. The maximum vertical displacement and horizontal displacement of the subgrade show an increasing linear trend with the number of vehicles. With the increase of the number of geogrids, the maximum vertical deformation of the subgrade changes little, and the maximum horizontal deformation of the subgrade changes significantly.

6. Discussion of Simulation Results of Geocell

6.1. Vertical Deformation and Horizontal Displacement. It can be seen from Figure 20 that the overall vertical deformation of the old subgrade is small and the change in the horizontal direction is not significant when geocells are set up. Under the condition of setting one and two layers of geocells, the vertical deformation of the new subgrade increases linearly with the distance from the center of the subgrade. With the three-layer geocell, the vertical deformation of the new subgrade increases linearly with the increase of the distance from the center of the subgrade, and the overall vertical deformation of the new subgrade is smaller than that of the old subgrade. Figure 21 shows the distribution rule of horizontal deformation of the top surface of the subgrade along the horizontal direction with a geocell. With the increase of the distance from the center of the subgrade, the horizontal deformation of the top surface of the subgrade shows a trend of increasing first and then becoming stable. Starting from the lap joint of the old and new subgrades, the horizontal deformation of the top surface of the subgrade tends to be stable.

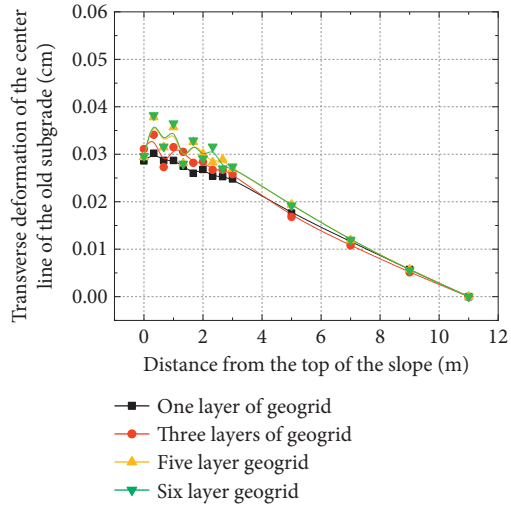

Figure 16: Variation rule of horizontal displacement along the depth of old subgrade center line.

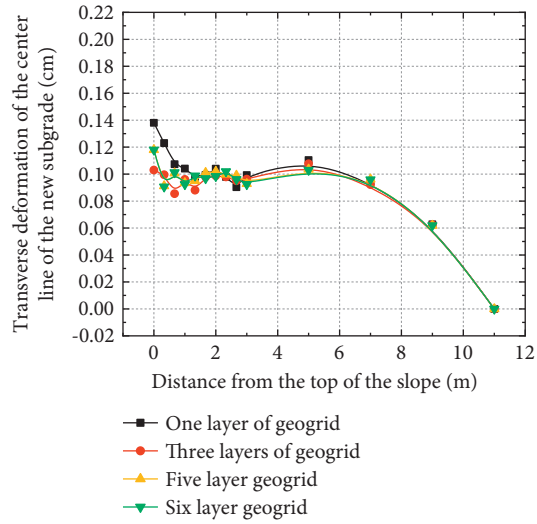

Figure 17: Variation rule of horizontal displacement along the depth of the new subgrade center line.

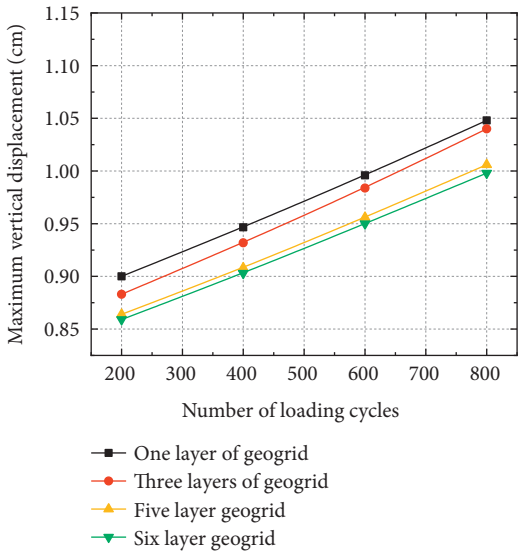

Figure 18: The rule of maximum vertical displacement of subgrade with the number of vehicles.

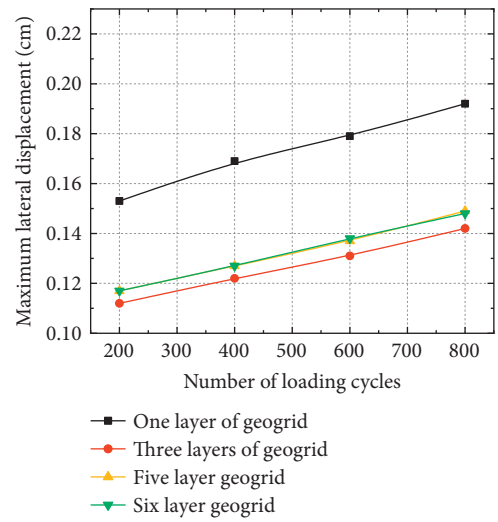

Figure 19: Maximum horizontal displacement of subgrade varies with the number of vehicles.

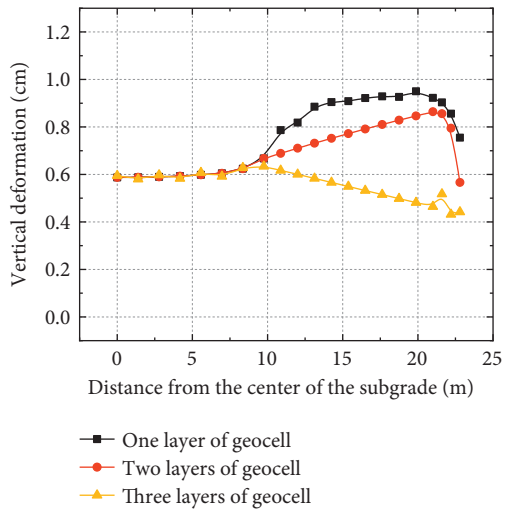

Figure 20: Vertical deformation rule of the top surface of subgrade along the horizontal.

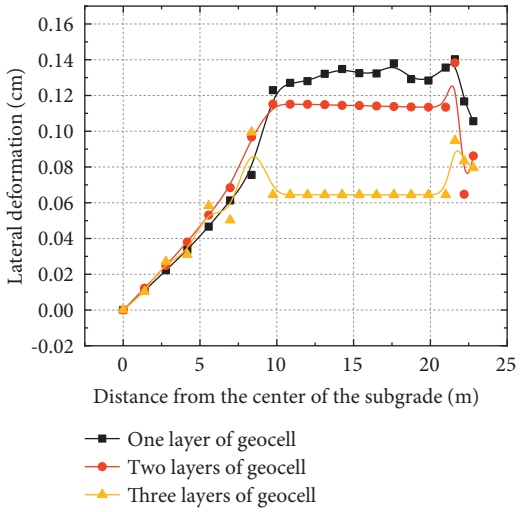

Figure 21: The rule of horizontal deformation of the top surface of subgrade along the horizontal direction.

6.2. Influence of Vehicle Number. It can be seen from Figures 22 and 23 that the maximum vertical displacement and maximum horizontal displacement of the subgrade increase linearly. With the increase of geocells, the maximum vertical deformation and maximum horizontal deformation of subgrade change obviously, the maximum vertical deformation decreases by 9.9% and 25.9%, and the maximum horizontal deformation decreases by 5.0% and 13.9%, respectively.

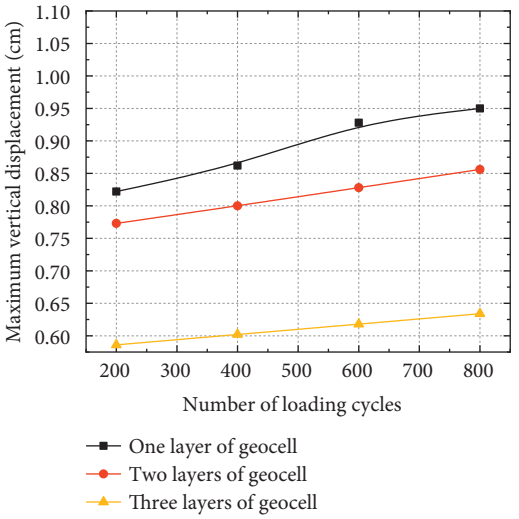

Figure 22: Vertical deformation.

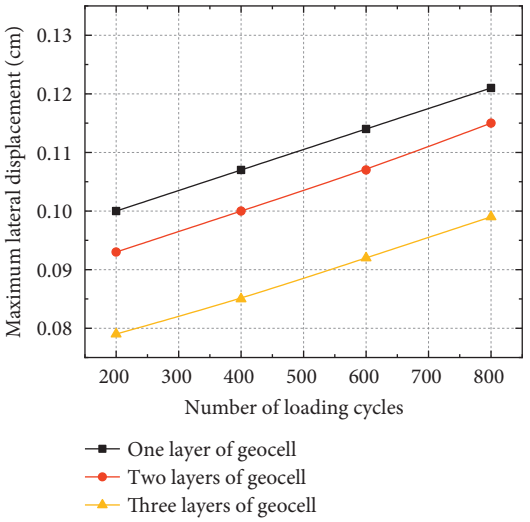

Figure 23: Horizontal deformation.

7. Conclusion

Highway widening has become an effective way to improve the carrying capacity of existing expressways. However, suppose the differential settlement between the new and the old subgrade is not controlled. In that case, it will lead to longitudinal cracks on the pavement, which will seriously affect the safety of vehicles. In this study, indoor tests were

carried out to study the variation of elastic modulus and dynamic elastic modulus of new and old subgrades under traffic load. A hyperbolic model of dynamic elastic modulus increasing with strain is proposed. The numerical calculation model of new and old subgrades under traffic load is established. The deformation characteristics of new and old subgrades without treatment measures and setting up geogrid and geocell are studied. The main conclusions are as follows:

(1) With traffic load and subgrade depth increase, the elastic modulus changes significantly in the early stage but has little changes in the later stage.

(2) With the increase of the distance from the center line of the subgrade, the vertical and horizontal deformation of the subgrade surface show a trend of increasing and then decreasing under the condition of no treatment measures. The maximum vertical deformation is in the center of the new subgrade, and the horizontal deformation is the most significant in the junction of the old and new subgrades.

Data Availability

The data used to support the findings of this study are included within the article. Any additional data related to the paper may be requested from the corresponding author.

Conflicts of Interest

The authors declare that they have no conflicts of interest.

Acknowledgments

This work was supported by the Science and Technology Plan of Shandong Transportation Department (grant no. 2019B48), the Shandong Key Research and Development Plan (grant no. 2019JZZY010429), and the Shandong Key Research and Development Plan (grant no. 2019GSF111040).

References

[1] H. H. Hung and Y. B. Yang, "Elastic waves in visco-elastic half-space generated by various vehicle loads," *Soil Dynamics and Earthquake Engineering*, vol. 21, no. 1, pp. 1–17, 2001.

[2] K. Knothe and S. L. Grassie, "Modelling of railway track and vehicle/track interaction at high frequencies," *Vehicle System Dynamics*, vol. 22, no. 3-4, pp. 209–262, 1993.

[3] L. S. Tang, P. Y. Lin, K. Wu, and X B. Deng, "Response characteristics of dynamic stress of subgrade soil under vehicle loads," *Yantu Gongcheng Xuebao/Chinese Journal of Geotechnical Engineering*, vol. 33, no. 11, pp. 1745–1749, 2011.

[4] A. Ahmed, T. U. Saeed, J. Murillo-Hoyos, and S. Labi, "Pavement repair marginal costs: accounting for heterogeneity using random-parameters regression," *Journal of Infrastructure Systems*, vol. 23, no. 4, 2017.

[5] M. Volovski, J. Murillo-Hoyos, and T. U. Saeed, "Estimation of routine maintenance expenditures for highway pavement segments: accounting for heterogeneity using random-effects models," *Journal of Transportation Engineering*, vol. 143, no. 5, pp. 11-12, 2017.

[6] T. U. Saeed, Y. Qiao, S. Chen et al., *Effects of bridge surface and pavement maintenance activities on asset rating,* Purdue University, Indiana, IN, USA, 2017.

[7] M. S. Yamany, T. U. Saeed, M. Volovski, and A. Ahmed, "Characterizing the performance of interstate flexible pavements using artificial neural networks and random parameters regression," *Journal of Infrastructure Systems*, vol. 26, no. 2, Article ID 04020010, 2020.

[8] L. S. Tang, P. Y. Lin, and K. Wu, "Elastic calculation model for dynamic additional stresses in layered subgrade under traffic load," *Chinese Journal of Rock Mechanics and Engineering*, vol. 28, no. 11, pp. 2208–2214, 2009.

[9] W. Cui, G. H. Lv, and C. Y. Liu, "Computational analysis of differential settlement on new subgrade in express way widening," *Science Technology and Engineering*, vol. 17, no. 34, pp. 326–331, 2017.

[10] Q. Bai, A. Ahmed, S. Labi, and K. C. Sinha, "Traffic volume benchmarks for major arterial widening versus expressway construction: exploratory approach," *Journal of Transportation Engineering Part A-Systems*, vol. 143, no. 8, Article ID 04017040, 2017.

[11] H. Qi, X. S. Zhang, J. Liu et al., "Study on deformation characteristics of low-highway subgrade under traffic load," *Applied Sciences*, vol. 12, no. 7, p. 3406, 2022.

[12] G. Li and Y. L. Guo, "Analysis on influencing factors of differential settlement of new and old subgrade in expressway reconstruction and extension," *Journal of Highway and Transportation Research and Development*, vol. 38, no. 7, pp. 22–28, 2021.

[13] W. G. Cao and T. Tan, "A prediction method of foundation settlement considering anomaly and newness-oldness degree influence boundedness of measured data," *Journal of Hunan University*, vol. 43, no. 3, pp. 37–43, 2020.

[14] J. C. Chai and N. Miura, "Traffic-load-induced permanent deformation of road on soft subsoil," *Journal of Geotechnical and Geoenvironmental Engineering*, vol. 128, no. 11, pp. 907–916, 2002.

[15] P. Bailly, F. Delvare, J. Vial, J. L. Hanus, M. Biessy, and D. Picart, "Dynamic behavior of an aggregate material at simultaneous high pressure and strain rate: SHPB triaxial tests," *International Journal of Impact Engineering*, vol. 38, no. 2-3, pp. 73–84, 2011.

[16] A. Flora, S. Lirer, and F. Silvestri, "Undrained cyclic resistance of undisturbed gravelly soils," *Soil Dynamics and Earthquake Engineering*, vol. 43, pp. 366–379, 2012.

[17] H. G. B. Allersma, L. Ravenswaay, and E. Vos, "Investigation of road widening on soft soil using a small centrifuge," *Transportation Research Record*, vol. 1462, pp. 47–53, 1994.

[18] X. L. Wen, C. Zhou, C. L. Li, and S P. Shang, "Large scale test on additional deformation of pavement widening with differential settlement," *China Journal of Highway and Transport*, vol. 26, no. 4, pp. 1–6, 2013.

[19] W. Q. Zhou, W. M. Leng, and D. G. Cai, "Analysis on characteristics of critical dynamic stress and accumulative deformation of coarse-grained soil subgrade filling under cyclic loading," *Tiedao Xuebao/Journal of the China Railway Society*, vol. 36, no. 12, pp. 84–89, 2014.

[20] L. Chen, J. Chen, and J. Zhang, "Test of dynamic properties of argillite-slate soil improved by cement," *Zhongnan Daxue Xuebao (Ziran Kexue Ban)/Journal of Central South University (Science and Technology)*, vol. 48, no. 7, pp. 1858–1865, 2017.

[21] X. D. Zhang and K. Ren, "Experimental study on dynamic elastic modulus and critical dynamic stress of cinder-improved soil subgrade," *Journal of Highway and Transportation Research and Development*, vol. 12, no. 4, pp. 25–32, 2018.

[22] Y. Y. Zhao, X. Z. Ling, Z. Y. Wang, X. Y. Shao, L. H. Tian, and G. Lin, "Test on dynamic characteristics of subgrade of heavy-haul railway in cold regions," *Sciences in Cold and Arid Regions*, vol. 7, no. 05, pp. 605–610, 2015.

[23] C. Dong, Z. Li, and Z. Yue, "Experimental study of dynamic characteristics of sand for highway subgrade," *Chinese Journal of Rock Mechanics and Engineering*, vol. 31, no. 1, pp. 3407–3412, 2012.

[24] L. Cong, Z. Guo, Q. Gao, and H. Zhang, "Permanent deformation characteristics and prediction model of silty subgrade soils under repeated loading," *Journal of Highway and Transportation Research and Development*, vol. 5, no. 2, pp. 22–26, 2011.

[25] H. F. Xing and H. M. Li, "Controlling criterion for differential settlement of widened expressway," *Applied Mechanics and Materials*, vol. 238, pp. 818–822, 2012.

[26] J. Liu, X. S. Zhang, G. H. Lv, K. Wang, B. Han, and Q. Xie, "Study on crack development of concrete lining with insufficient lining thickness based on czm method," *Materials*, vol. 14, no. 24, p. 7862, 2021.

[27] J. Wei, Z. Wang, J. Zheng, and W. Zhao, "The finite element analysis of highway unilateral widened deformation characteristics on soft soil ground," *Advanced Science Letters*, vol. 6, no. 1, pp. 337–341, 2012.